Single-phase and Three-phase Compatible T-type AC-DC Converter for Active Power Decoupling

Ryohei Higashide¹, Hiroki Watanabe¹, Jun-ichi Itoh¹

¹ Nagaoka University of Technology

Abstract - This paper focuses on the theoretical harmonic analysis of a single-phase and three-phase compatible T-type AC-DC converter with active power decoupling (APD). The APD causes harmonics near the switching frequency in the converter input voltage. This paper derives the converter input voltage when APD is applied using a double Fourier series and presents the theoretical basis for filter optimization. Simulation results confirm the validity of the theoretical analysis.

Keywords On-board charger, T-type AC-DC converter, Single-phase and three-phase compatible, Active power decoupling

I. Introduction

In recent years, single-phase and three-phase compatible on-board chargers(OBCs) for electric vehicles have been actively researched [1]. These power converters can utilize the built-in leg during single-phase grid operation in order to apply the active power decoupling (APD) function. In particular, the APD method using a T-type AC-DC converter requires no additional circuitry. However, since the DC-side capacitor pulsates due to the APD, the converter's input voltage exhibits a harmonic spectrum of switching frequency components despite the multilevel converter configuration.

This paper mathematically derives the converter input voltage when applying the APD for optimal filter design using a double Fourier series.

II. Single-phase and Three-phase Compatible T-type AC-DC Converter

Fig. 1 shows the circuit configuration of the single-phase and three-phase compatible T-type AC-DC converter. The system functions as a T-type AC-DC converter and a half-bridge APD circuit by connecting the w-phase terminal T3 to the neutral point of the DC-side capacitor T4. This configuration achieves APD during single-phase system operation without requiring additional circuitry. Fig. 2 shows the block diagram for single-phase grid operation. As shown in Fig. 2(a), conventional carrier level-shift modulation is applied to the T-type AC-DC converter. The APD circuit includes two main control functions: capacitor voltage balancing and neutral point current control, as shown in Fig. 2(b). Neutral point current control functions to pulsate the capacitor voltages for the APD. These voltages are expressed

$$\begin{cases} v_{c1} = \frac{V_{dc}}{2} + V_{c} \sin(\theta - \frac{\pi}{4}) \\ v_{c2} = \frac{V_{dc}}{2} - V_{c} \sin(\theta - \frac{\pi}{4}) \end{cases}$$
 (1),

where $V_{\rm dc}$ is the DC bus voltage, $V_{\rm c}$ is the amplitude of the capacitor voltages, and θ is the grid angle.

III. Theoretical Harmonic Analysis

The converter input voltage $v_{\rm rec}$ with APD exhibits a harmonic spectrum near the switching frequency despite the multilevel converter configuration. This is caused by the DC-side capacitor pulsating due to the APD. Therefore, the filter design method differs from that of typical multilevel converters. Since the harmonics depend on the design value of the capacitor voltage amplitude, theoretical harmonic analysis is required for optimal filter design.

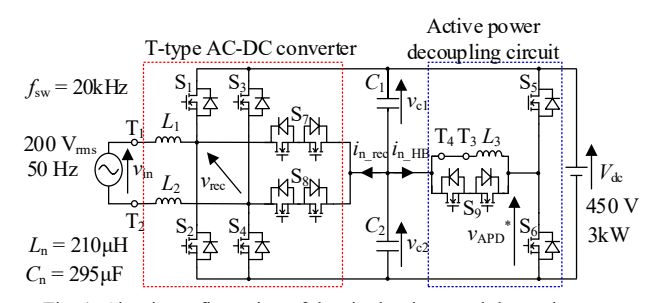
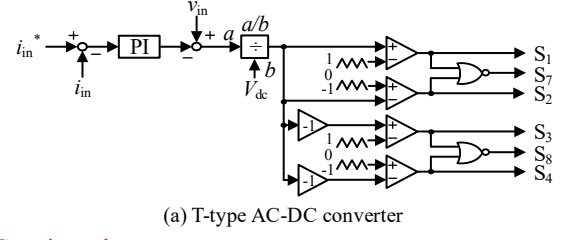
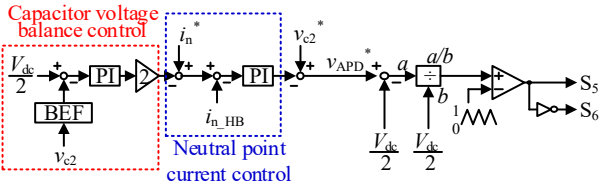


Fig. 1. Circuit configuration of the single-phase and three-phase compatible T-type AC-DC converter in single-phase grid operation.





(b) Active power decoupling circuit

Fig. 2. Block diagram in single-phase grid operation.

Fig. 3 shows the voltage contour plot of the u-phase measured from the neutral point. The vertical axis represents the angle of the triangular carrier, and the horizontal axis represents the angle of the reference waveform. Each axis sets the peak of each waveform to 0 degrees. Calculating $v_{\rm un}$ using a double Fourier series from Fig. 3, the converter input voltage $v_{\rm rec}$ is expressed as

$$\begin{split} &v_{\rm rec} = v_{\rm un} - v_{\rm vn} = V_{\rm dc} M \cos \theta \\ &+ \frac{2\sqrt{2}V_{\rm c}}{\pi} \sum_{m=1}^{\infty} \frac{1}{2m-1} \sum_{n=-\infty}^{\infty} J_1 \big\{ (2m-1)\pi M \big\} \cos \big\{ (2m-1)\theta \big\} \\ &+ \frac{2V_{\rm c}}{\pi} \sum_{m=1}^{\infty} \frac{1}{2m-1} \sum_{n=-\infty}^{\infty} \left[A_{\rm mn} \cos \big\{ (2m-1)\theta + 2n\theta_{\rm c} \big\} \right] \\ &+ \frac{2V_{\rm dc}}{\pi} \sum_{m=1}^{\infty} \frac{1}{2m} \sum_{n=-\infty}^{\infty} J_{2n+1} \big\{ 2m\pi M \big\} \cos \big\{ 2m\theta + (2n+1)\theta_{\rm c} \big\} \end{split}$$
(2),

where

$$A_{mn} = (-1)^n \left\{ J_{2n+1} \left\{ m\pi M \right\} - J_{2n-1} \left\{ m\pi M \right\} \right\}$$

$$B_{mn} = (-1)^n \left\{ J_{2n+1} \left\{ m\pi M \right\} + J_{2n-1} \left\{ m\pi M \right\} \right\}$$

$$(3),$$

and where M is the modulation index, θ_c is the carrier angle, J_n is the Bessel function of the first kind. Note that v_{vn} is calculated by shifting the phase of the reference waveform by 180 degrees.

IV. Simulation Results

The simulation conditions are also shown in Fig.1. The voltage amplitude and capacitance of the DC-side capacitor are set to 180 V and $295 \mu\text{F}$, respectively.

Fig. 4 shows the simulation waveforms in a steady state. Fig. 4(a) shows that $v_{\rm rec}$ is similar to the waveform of a typical multilevel converter since APD is not applied. The input current THD without applying APD is 0.95% (up to $40^{\rm th}$ order). However, Fig. 4(b) shows pulsating DC-side capacitor voltage since APD is applied. As a result, harmonic components are superimposed on the converter input voltage $v_{\rm rec}$. This also increases the ripple in the input current. Consequently, the current THD is 0.96% (up to $40^{\rm th}$ order).

V. Validation of the Theoretical Equation

Fig. 5 shows the comparison of the theoretical value and simulation result for the harmonic analysis of converter input voltage $v_{\rm rec}$. The vertical axis represents the amplitude of each harmonic normalized to the fundamental component. Fig. 5(a) shows the harmonic spectrum appearing only near even multiples of the switching frequency without APD. This result is similar to that of typical multilevel converters. On the other hand, Fig. 5(b) shows a harmonic spectrum appearing also near odd multiples of the switching frequency due to the APD. Fig. 5 shows the amplitudes match between the theoretical values and the simulation result. This result demonstrates the accuracy of the harmonic theoretical equation when applying the APD.

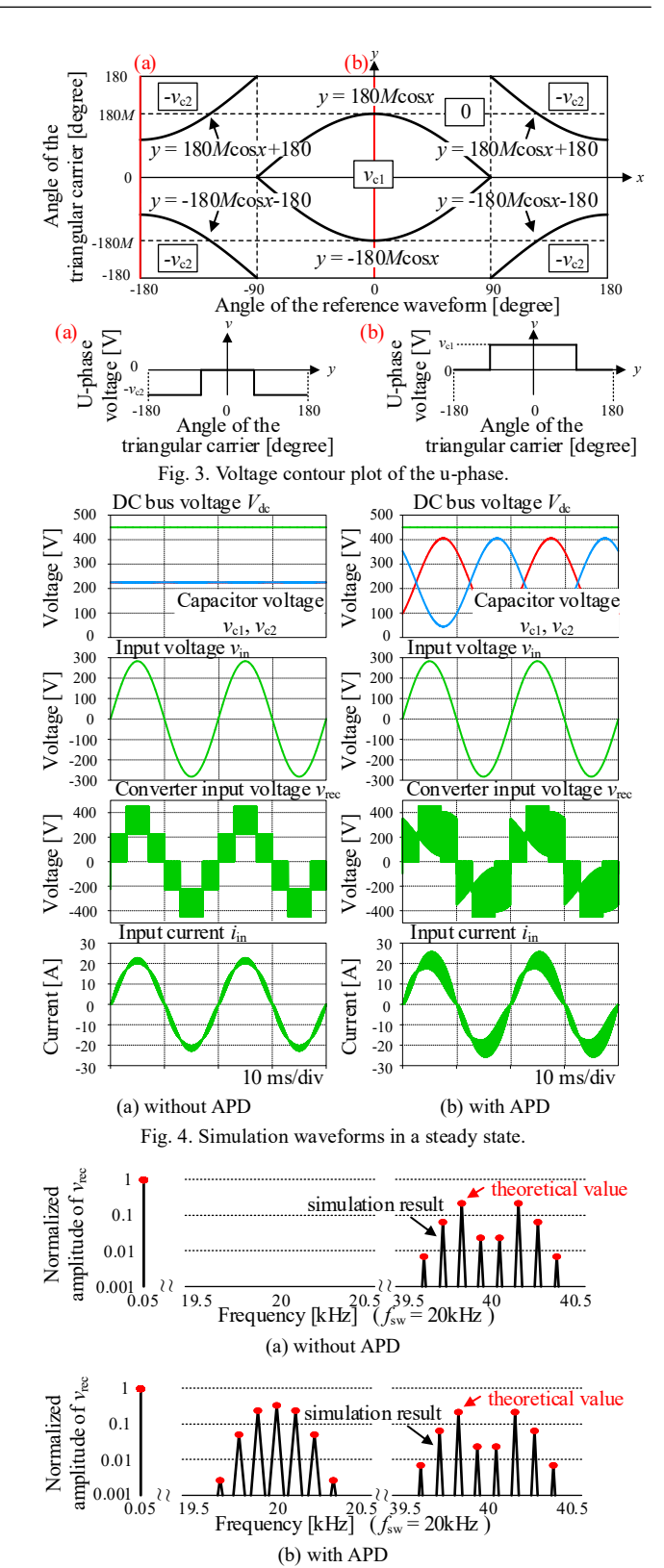


Fig. 5. Comparison of theoretical value and simulation result for harmonic analysis in converter input voltage v_{rec} .

References

[1] H. Zhao et al: "A Single- and Three-Phase Grid Compatible Converter for Electric Vehicle On-Board Chargers" in *IEEE Transactions on Power Electronics*, vol. 35, no. 7, pp. 7545-7562, July 2020